AUTONOMOUS ECO-DRIVING WITH TRAFFIC LIGHT AND LEAD VEHICLE CONSTRAINTS:AN APPLICATION OF BEST CONSTRAINED INTERPOLATION

Yara Hazem Mohamed Mahmoud, M.S.

Western Michigan University, 2022

Eco-Driving is a critical technology for improving automotive transportation efficiency. It is achieved by modifying the driving trajectory over a particular route to minimize required propulsion energy. Eco-Driving can be approached as an optimal control problem subject to driving constraints such as traffic lights and positions of other vehicles. Best interpolation in a strip is a problem in approximation theory and optimal control. The solution to this problem is a cubic spline. In this research we demonstrate the connection between Eco-Driving and best interpolation in the strip. By exploiting this connection, we are able to generate optimal Eco-Driving trajectories that could be driven with an autonomous system. Using the simulation tool FASTSim, we can evaluate the trajectories using conventional, hybrid electric, and fully electric vehicle models. Our results quantify the energy efficiency improvements that can be achieved with the proposed approach.

AUTONOMOUS ECO-DRIVING WITH TRAFFIC LIGHT AND LEAD VEHICLE CONSTRAINTS:AN APPLICATION OF BEST CONSTRAINED INTERPOLATION

by

Yara Hazem Mohamed Mahmoud

A thesis submitted to the Graduate College
in partial fulfillment of the requirements
for the degree of Master of Science
Mathematics
Western Michigan University
April 2022

Thesis Committee:

Melinda Koelling, Ph.D., Chair
Zachary D. Asher, Ph.D.
Jim Zhu, Ph.D.

ACKNOWLEDGMENTS

I would like to thank my thesis Advisor,Dr Melinda Koelling for helping me to get to do a thesis-based masters and start a program from scratch, Dr Asher for believing in me and taking me in his lab when no one else did, The EEAV lab graduate students for being with me in my journey and helping me out whenever they can.

I would like to thank especially Dr Ziebarth (Chair of the Math Department) for providing me the funds needed to complete my education. Without this fund I would not have been able to focus on my work and I would have struggled financially.

My parents and friends who bore my crying nights and anxiety.My mom's and grandma's prayers, Noha who helped me throughout my first year of college, Mariam, who was my partner in crime from day one and college and graduate school sucks without her, and Matthew who is still helping me with Linear Algebra class.

last but not least, I would like to thank my self for getting me to this point of education and being determined to achieve my dreams. It has not been all pink and white, I had some grey and black days, however I was determined to prove myself and I did.

Yara Hazem Mohamed Mahmoud

TABLE OF CONTENTS

LIST OF TABLES

LIST OF FIGURES

LIST OF ABBREVIATIONS

CAFE	Corporate Average Fuel Economy
CV	Conventional Vehicle
EEAV lab	Energy Efficiency and Autonomous Vehicles lab
Ego Vehicle	Testing Vehicle
EPA	Environmental protection agency
EV	Electric Vehicle
FASTSim	Future Automotive Systems Technology Simulator
FE	Fuel Economy
HEV	Hybrid Electric Vehicle
KA	Kalamazoo Arterial
KD	Kalamazoo Downtown
Lead Vehicle	Upper limit (speed) constraint
MPGge	Mileage per gallon gasoline equivalent
MPG	Mileage per gallon
SPaT	Signal Phasing and Timing
V2I	Vehicle-to-Infrastructure
V2V	Vehicle-to-Vehicle

CHAPTER 1

INTRODUCTION

In the United States., the National Highway Traffic Safety Administration's (NHTSA) Corporate Average fuel economy (CAFE) requirement is gradually raised on an annual basis to reduce the adverse consequences of automotive transportation (1). These adverse consequences include economic costs for petroleum importation and vulnerability to geopolitical stability (2), accelerated global warming due to large amounts of greenhouse gas emissions (3), and adverse effects on human health due to air pollution (4; 5). To date, the CAFE policy has been shown to be effective in promoting energy efficiency technology in modern commercially-available vehicles (6).

1.1 Literature Review

In 1977, Schwarzkopf first demonstrated the fuel economy in road vehicles does not only depend on the drive train but also on the driving pattern (7). Schwarzkopf algorithm was derived from the Pontryagin Maximum Principle to provide a mathematically optimal driving performance subject to the driver's trip time limit. In 1993, Dontchev introduced the problem of the best interpolation in a strip. Dontchev proved that the solution to his problem is a cubic spline which depends continuously on the data. In 1995, Dontchev and Kolmanovsky presented a method for the reduction of best interpolation in a strip to an unconstrained minimization problem that can be used in many optimization applications (8).

In 2001, Ericsson (9) showed that different driving patterns have different effects on vehicle emissions and fuel consumption. In 2012, the National Renewable Energy Laboratory researchers showed that implementing Eco-Driving behavior results in fuel economy improvements (10). In 2014, researchers at the University of Minnesota applied a traffic light model to predict future vehicle velocity with vehicle-to-vehicle (V2V) and vehicle-to-infrastructure (V2I) technologies as

inputs (11). Their research employed Pontryagin's Minimization Principle which resulted in an improvement in the fuel economy (FE) with the prediction-with-error scenario. Starting in 2018, researchers at Colorado State University utilized a speed prediction method utilizing simulated V2V communication with real-world driving data and a drive cycle database to improve Vehicles FE using a predictive energy management system (12).

Additionally, research that was conducted at the University of Michigan and then transitioned to Western Michigan University continued to investigate and exploit further methods to improve FE using different control methods. In 2020, Western Michigan University Energy efficient and Autonomous Vehicles (EEAV) lab and the Department of Mathematics collaborated with the University of Michigan researchers to apply the " Best interpolation in a strip " problem to a real-life application that resulted in this research.

1.2 Importance of Eco-Driving

Eco-Driving is an effective method of achieving significant energy efficiency improvements in vehicles. Eco-Driving is the realization of a more energy-efficient drive cycle for a given route. It is typically achieved by eliminating full stops, maintaining a constant speed, limiting acceleration, and smoothing the velocity profile (10) (13) (14). Implementing energy-efficient driver behavior reduces the vehicle propulsion energy required to drive the route.

Energy-efficient driver behavior typically results in longer travel time and it has historically lower user acceptance by human drivers (10). However, human driver resistance may be reduced when combined with driving automation technologies. Automation technologies, such as advanced driving assistance systems (ADAS) and autonomous vehicles (AV) have high user acceptance (15), and it is likely that users can look past the increased travel time from Eco-Driving in exchange for not having to do all the driving.

Recent research has shown that when implementing a heuristic set of goals such as removing stops, traveling at an energy-efficient speed (in general, this could be a higher or lower overall speed), and limiting acceleration and deceleration magnitudes, it is possible to achieve Fuel Economy (FE) improvements of approximately 10% for modern vehicles and 30% for fully autonomous vehicles (13). Also, when Eco-driving is applied to electrified vehicles the result is longer battery-

life and slower battery degradation (16). Additionally, vehicles without Eco-Driving technology can still improve their energy efficiency if they follow an Eco-driving equipped lead vehicle (17).

The problem of maximizing the energy efficiency improvements from Eco-Driving can be formulated as an optimal control problem if a prediction of driving conditions along the route, such as traffic lights and traffic positions, are available. These predictions are informed by vehicle sensors and vehicle to vehicle (V2V) and vehicle to infrastructure (V2I) communication technologies. As an example of a typical Eco-Driving study, predictions of traffic light signal phase and timing (a V2I technology) were used to change driving behavior and demonstrated a fuel economy improvement of 12-14% (18).

Another study showed that using V2I-enabled traffic lights decreases the energy consumed in Eco-Driving (17). Other approaches include the optimization of speed and power distribution between the motor and engine in a connected HEV subject to A/C thermal load (19), imposing constraints on vehicles that are queued for a green light (20; 21), and using information from the vehicle in front and traffic light data to avoid red lights (22). Additionally, applications of Model Predictive Control (MPC) and Dynamic Programming (DP) have been considered in a lead vehicle following scenario (23). Other connections between control theory and spline interpolation are illustrated in (24).

1.3 Research Goals and Contribution

Our approach here is unique compared to the past efforts because we demonstrate a connection between Eco-Driving and a problem in approximation theory and optimal control (25; 26). This problem is called "best interpolation in a strip". By exploiting this connection, we show that it is possible to quickly generate optimal Eco-Driving trajectories for real-world driving scenarios with traffic lights and lead vehicle constraints. As expected, these derived optimal trajectories show significant energy efficiency improvements when used in real-world validated models and compared to EPA reported FE.

After this chapter, we proceed as follows.

In Chapter 2, we first state the methodology where assumptions are explained, the problem is formulated graphically, and the optimal control solution derivation and possible solutions to

the problem explained. Furthermore, we go over the implementation of the problem algorithm on different routes and using different vehicle architecture. In Chapter 3, we study the Optimal control solution and the resulting FE and compare these results to the EPA FE for a city route. Finally, we conclude our research in Chapter 4 and discuss further research.

CHAPTER 2

METHODOLOGY

We consider a problem of generating an Eco-Driving trajectory subject to real-world driving constraints of traffic lights and avoiding collisions with a lead vehicle. Since precise vehicle control is required, this has primary applications in autonomous or assisted control rather than human driver control.

2.1 Problem Statement and Assumptions

Several assumptions are made:

1. **Vehicle trajectory is to be specified as a function of time**
   Specifically, we assume that we are able to maintain precise control of the subject vehicle (ego vehicle) velocity on a second-by-second basis, which would be enabled by autonomous or assisted vehicle control.

2. **Minimizing the integral of the square of the acceleration over time increases energy efficiency**
   Previous research into Eco-Driving suggests that the Eco-Driving can be achieved without high-fidelity models of vehicle fuel consumption; instead, it is sufficient to minimize acceleration (23; 27; 28) and, whenever possible, pass through the traffic lights when they are green to avoid braking, stopping and idling. This approach is adopted in this paper as well.

3. **Piece-wise linear lead vehicle constraint**
   We further assume that the ego vehicle is following a lead vehicle which is represented here with a simple piecewise linear distance vs. time function.

4. **Asynchronous SPaT along a straight drive cycle**

   We consider asynchronous traffic light signal phase and timing (SPaT) along a straight route during which the ego vehicle will stop for red lights.

Noting that the optimal solution to this problem would be driven towards extremely low speeds which is impractical for real world applications. To combat this tendency, we will impose an additional constraint on travel time to ensure that the vehicle is not a traffic hazard. These assumptions lead to an optimal control formulation which is also linked to a problem in approximation theory: the best interpolation in a strip.

2.2 Optimal Control Problem Formulation

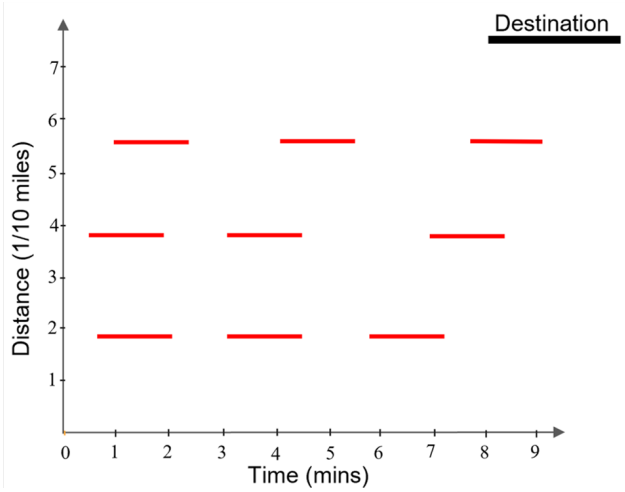

Figure 2.1: Visualization of SPaT data of 3 traffic lights where red dashes indicate when each light is red. Traffic lights are located approximately 1.9, 3.9, and 5.7 tenth of a mile.

To visualize how the optimal control problem is formulated, time is represented by the x-axis in minutes and distance by the y-axis in a tenth of mile increments. Three traffic lights are used to represent the red-light phase (Fig.2.1), where the first traffic light occurs at 0.19 miles and lasts for almost a minute. The lead vehicle trajectory is forecasted as the upper constraints, represented by the blue line (Fig.2.2). To assure that the ego vehicle always arrives at the traffic intersection before the light turn red, a lower constraint, represented by the pink line, is forecasted; it bounds the trajectory window to include time and location just before the traffic light turns red

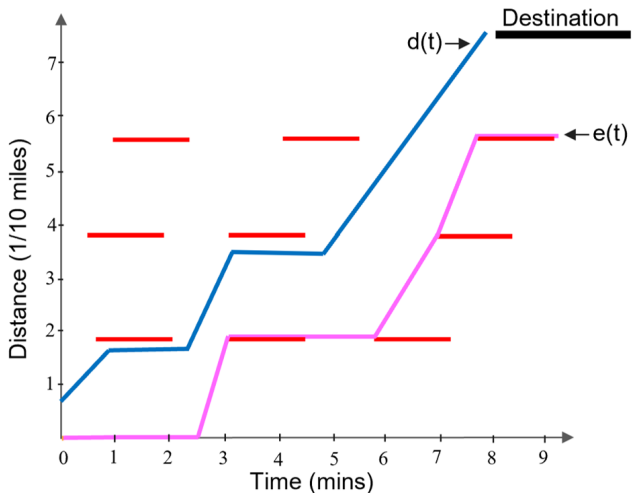

Figure 2.2: In (blue) trajectory of forcasted lead vehicle travelling at speed limit and stops at any red light it encounters. In (pink) the trajectory window just before the traffic light turn red.

but not include red lights in the interior of the trajectory window (Fig.2.2). It can be seen that the lead vehicle stopped at the first red light phase of the first traffic light, then stopped for almost the entire duration of the second red light phase of the second traffic light, and, finally, encountered the third traffic light in a green phase and thus drove through the intersection.

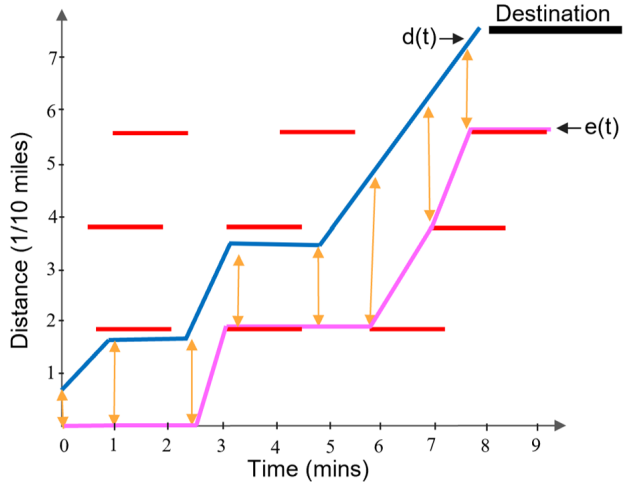

Figure 2.3: Visualization of the gates (double-ended arrows) that constrain the location of the ego vehicle.

Consider now the ego vehicle's position vs time, $f(t)$. The location of the ego vehicle is represented by waypoints. These waypoints lie somewhere within the corresponding gates delin-

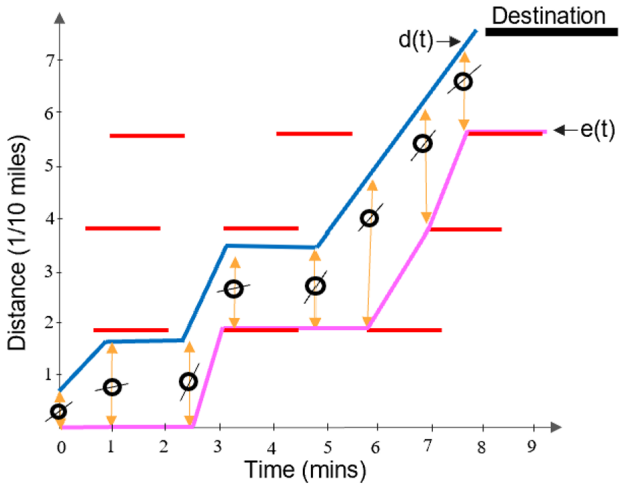

Figure 2.4: Visualization of the location of waypoints (black circles) and velocity of the ego vehicle (slope of strike through black lines).

eated by orange double ended arrows (Fig. 2.3). These gate locations are set based on changes in boundary conditions (e.g. the lead vehicle transitions from zero velocity to some constant velocity). Where $f(t)$ has to connect the waypoints which are designated by black circles in Fig. 2.4, the ego vehicle velocities at each waypoint are indicated by black lines. The waypoint locations, the vehicle velocities at the waypoints, and the trajectory "pieces" between the waypoints are determined by the theory of best interpolation in a strip.

Fig. 2.5 shows a visualization of the distance vs time problem geometry with SPaT data of three traffic lights, lead vehicle trajectory ($d(t)$, blue line) and the trajectory window just before the traffic light turns red ($e(t)$, pink line). Note that the lower constraint, $e(t)$, is determined based on trailing red light SPaT phases (in other words, the ego vehicle must pass through each intersection before the light turns red).

By assigning the orange markers as "gates", we can now designate the interval between gates as the "strip". Shown in the inset dashed green circle in Fig. 2.5 is a strip where the left boundary (the start time of the strip) is designated as t_i and the right boundary (the end time of the strip) is designated as t_{i+1}. The ego vehicle position at certain time instant $f(t_i)$, where i is the discrete time step index, is bounded above by $d(t_i)$ and below by $e(t_i)$. Overall, the ego vehicle trajectory has to adhere to the following constraints:

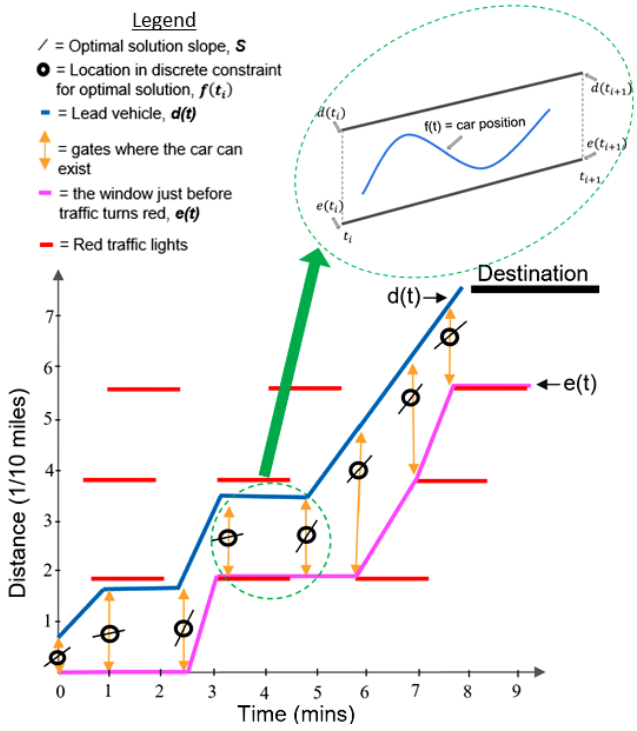

Figure 2.5: General problem geometry showing in the green dashed circle a zoomed in strip between $t_i = 3.1$ and $t_{i+1} = 4.8$ mins, the lead vehicle $d(t)$, red light phase constraint $e(t)$.

1. $f(t) \leq d(t)$, where $d(t)$ is informed by the forecasted lead vehicle position offset by safety margin;

2. $f(t) \geq e(t)$, where $e(t)$ is informed by the transition of the traffic signal phase to red.

3. Left: Start of the time interval $\rightarrow t_i$

4. Right: End of the time interval $\rightarrow t_{i+1}$

Note that constraints $e(t) \leq f(t) \leq d(t)$ form a strip that has two gates in distance vs. time that the ego vehicle must pass through similar to the way a slalom skier passes through gates during a competition. However, unlike a slalom skier, who pursues a minimum time trajectory, we seek to minimize the L_2 norm of the ego vehicle acceleration trajectory which in turn improves energy efficiency.

The constraints $e(t)$ and $d(t)$ are assumed to be piecewise linear; they are linear functions of time in each time interval $[t_i, t_{i+1}]$, where the time intervals are fixed. There are a few caveats

regarding this. Firstly, for real-world lead vehicles, this corresponds to an approximated representation. The theory of best interpolation in a strip does allow for piecewise cubic constraints which could be incorporated in future research. Secondly, the continuity of $e(t)$ is enforced by not allowing infinite slope in the $e(t)$ function as can be seen in Fig. 2.5. Lastly, it should also be mentioned that realistically, the $d(t)$ constraint should include a distance margin from a lead vehicle.

To demonstrate the concept of this research, we will use the routes shown in Figs. 2.6 and 2.7 with their associated real-world red light locations and speed limits. We will designate the Fig. 2.6 route as Kalamazoo Arterial (KA) and the Fig. 2.7 route as Kalamazoo Downtown (KD).

For these routes, real world vehicle velocity was recorded along two different roads in Kalamazoo, MI: one along Stadium drive to serve as the arterial route and one along Kalamazoo Mall to serve as the downtown route. A consistent SPaT cycle of 120 seconds was used for this demonstration since it represents a broad use case (29; 30). This SPaT data then informs specific piecewise linear upper and lower constraints for the optimal control problem. We note that the lead vehicle constraints in this paper are defined by speed limits and converted to piecewise linear functions. Based on results in (25; 8; 26), piecewise cubic constraints can also be handled, but this is left to future work.

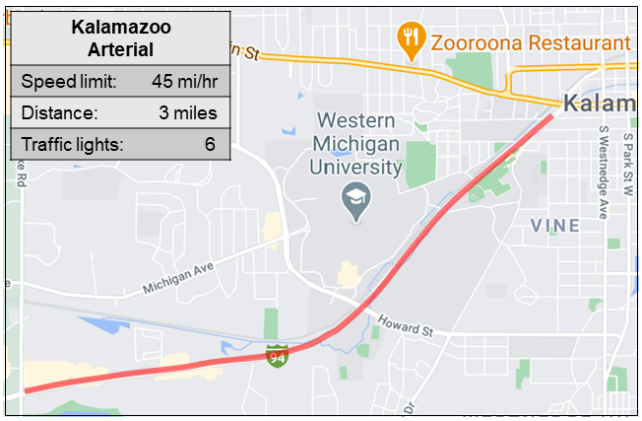

Figure 2.6: Details of the Kalamazoo Arterial route which is used to collect lead vehicle and SPaT data contraints.

In the above and subsequent developments we assumed that there is either no vehicle trailing the ego vehicle, or such a trailing vehicle does not influence the ego vehicle trajectory. In principle, this assumption could be relaxed, e.g., the lower constraint on the ego vehicle trajectory

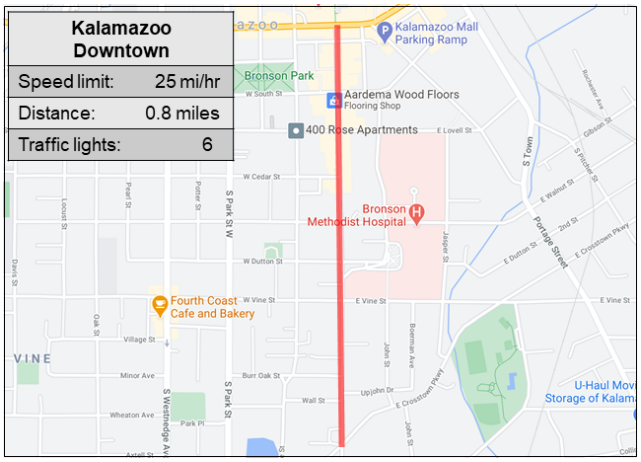

Figure 2.7: Details of the Kalamazoo Downtown route which is used to collect lead vehicle and SPaT data contraints.

can be additionally informed by a trailing vehicle trajectory in order to minimize disruption to its motion.

2.3 Optimal Control Solution

The eco-driving problem set-up exploits the connection with the problem of best interpolation in a strip (25; 8; 26). In particular, the planning of vehicle distance trajectory versus time, $f(t)$, $t_0 \le t \le t_N$, can be posed as the following problem:

Given time instants $t_0 < t_1 \cdots < t_N$, initial and final slopes s_0 and s_N, lower and upper bounding functions e and d satisfying $e(t) < d(t)$ for all $t \in [t_0, t_N]$ which are continuous on $[t_0, t_N]$, and linear on $[t_i, t_{i+1}]$, determine the function f that satisfies the following optimization problem:

$$\begin{aligned} &\underset{f(\cdot)}{\text{Minimize}} \quad \|f''\|_{L^2_{[t_0,t_N]}} \\ &\text{subject to} \\ &\qquad e(t) \le f(t) \le d(t), \quad t_0 \le t \le t_N, \\ &\qquad \dot{f}(t_0) = s_0, \quad \dot{f}(t_N) = s_N. \end{aligned} \tag{2.1}$$

The computational approach to finding such a function f then decomposes into an outer

and an inner optimization problems. The outer loop problem is to minimize the function

$$\phi(y,s) = \sum_{i=0}^{N-1} \phi_i(y_i, s_i, y_{i+1}, s_{i+1}), \tag{2.2}$$

where $y = (y_0, \cdots, y_N)$ and $s = (s_0, \cdots, s_N)$ are vectors of function values and slopes at t_i where y_0, y_N, s_0 are predetermined constants, $s_N = 0$ indicating the ego vehicle comes to a full stop at the end of the trip , $i = 0, \cdots, N$, and $\phi_i(y_i, s_i, y_{i+1}, s_{i+1})$, $i = 0, \cdots, N-1$ are computed by solving N independent inner optimization problems:

$$\begin{aligned} &\underset{f(\cdot)}{\text{Minimize}} \ \ \|f''\|_{L^2_{[t_i, t_{i+1}]}} \\ &\text{subject to} \\ &\qquad f(t_i) = y_i, \quad f(t_{i+1}) = y_{i+1} \\ &\qquad \dot{f}(t_i) = s_i, \quad \dot{f}(t_{i+1}) = s_{i+1} \\ &\qquad e(t) \le f(t) \le d(t), \quad t_i \le t \le t_{i+1}. \end{aligned} \tag{2.3}$$

The function ϕ can be shown to be a convex and coercive function of the arguments y and s, and it has a unique minimum (25; 8; 26). The solution to the inner loop optimization problem (2.3) is a C^2 cubic spline that is one of the following types determined by its interactions with the lower and upper constraining functions $e(t)$ and $d(t)$, $t_i \le t \le t_{i+1}$:

Case 1: Constraints are inactive;

Case 2: Single touching point on the lower constraint e;

Case 3: Single touching point on the upper constraint d;

Case 4: Single subarc on the lower constraint e;

Case 5: Single subarc on the upper constraint d;

Case 6: Touching pair with the first touching point on the lower constraint e and second touching point on the upper constraint d;

Case 7: Touching pair with the first touching point on the upper constraint d and second touching point on the lower constraint e.

Note that when y_i, y_{i+1}, s_i and s_{i+1} are given, the optimal trajectory of (2.3) is unique and corresponds to one of the cases 1-7. In order to find this optimal trajectory we evaluate the cost for each of the cases for which a feasible solution exists and select the case corresponding to the minimal value. The construction of these solutions involves solving a system of linear algebraic equations for the coefficients of a piecewise cubic polynomial. In that sense problem (2.3) is solved as a combinatorial optimization problem.

The candidate solutions of the 7 cases are in the form of one of the below 4 different systems of equations. In some cases knots are added, which are determined by the points of intersection of $f(t)$ and the upper or lower bounds. Mathematically, a knot represents the transition between cubics.

Case 1: the constraints are not active (no knots added);

$$f_1(t) = k_1(t-t_i)^3 + k_2(t-t_i)^2 + k_3(t-t_i) + k4 \tag{2.4}$$

In case 1, Fig. 2.8, there is no active constraints where there are no additional knots other than the fixed knots $[t_i, t_{i+1}]$. The optimal solution is $f(t)$ which is the vehicles trajectory between the lower, $e(t)$, and upper, $d(t)$, constraints.

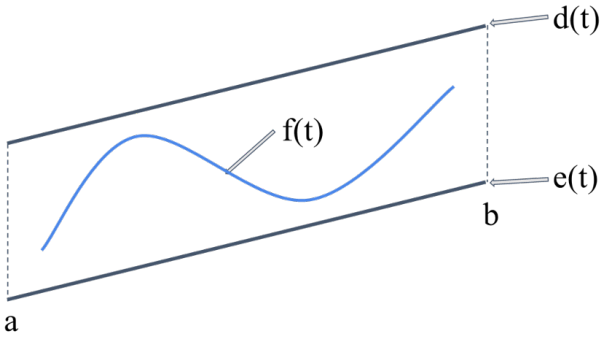

Figure 2.8: No active constraints definition, where $a = t_i$ and $b = t_{i+1}$.

Case 2 & 3: a single touching point on one of the constraints (one additional knot);

$$f_2(t) = \begin{cases} k_l(\delta - t)^3 + k_2(\delta - t)^2 \\ \qquad + k_3(\delta - t) + k4 \\ \qquad\qquad t \in [t_i, \delta] \\ m_l(-\delta + t)^3 + m_2(-\delta + t)^2 \\ \qquad + m_3(-\delta + t) + m_4 \\ \qquad\qquad t \in [\delta, t_{i+1}] \end{cases} \tag{2.5}$$

The case, Fig. 2.9, with one the Eco-Vehicle, $f(t)$, hitting the upper, $d(t)$, or lower, $e(t)$, constraint. Reaching this case would cause the Eco-Vehicle to decelerate and accelerate over a given amount of time to maintain optimal solution.

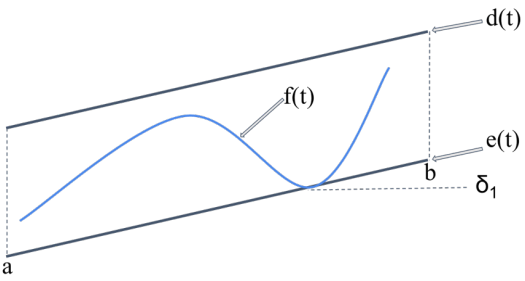

(a) single touching point on lower constraint

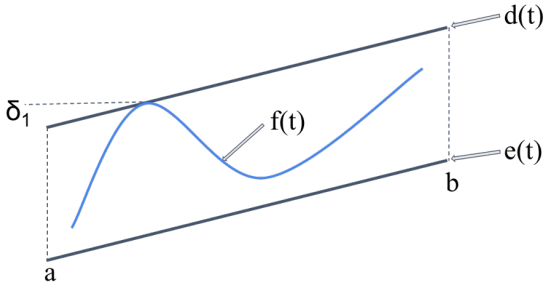

(b) single touching point on upper constraint

Figure 2.9: Single touching point definition, where $a = t_i$ and $b = t_{i+1}$.

Case 4 & 5: a sub-arc on one of the constraints (two additional knots);

$$f_3(t) = \begin{cases} k_l(\delta_1 - t)^3 + k_2(\delta_1 - t)^2 \\ \qquad + k_3(\delta_1 - t) + k4 \\ \qquad\qquad t \in [t_i, \delta_1] \\ e(t) \qquad\qquad t \in [\delta_1, \delta_2] \\ m_l(-\delta_2 + t)^3 + m_2(-\delta_2 + t)^2 \\ \qquad + m_3(-\delta_2 + t) + m_4 \\ \qquad\qquad t \in [\delta_2, t_{i+1}] \end{cases} \tag{2.6}$$

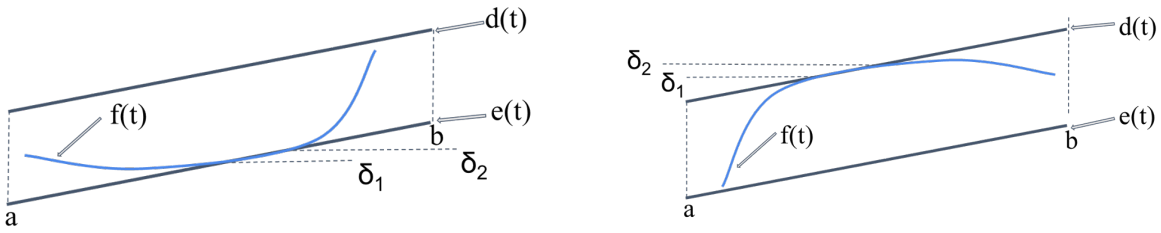

(a) single subarc on lower constraint

(b) single subarc on upper constraint

Figure 2.10: Two touching points, subarc, definition, where $a = t_i$ and $b = t_{i+1}$.

These cases, Fig. 2.10, cause a sub-arc to touch the upper, $d(t)$ or lower, $e(t)$, limit. This trajectory can simulate a vehicle following the lead vehicle in traffic or possibly the speed limit while not speeding to maintain optimal FE in order to avoid an upcoming stop light in traffic. This must happen to make sure the $v > 0$ to avoid stop lights. In our test it is unlikely that the solution will contact the lower constraint $e(t)$ to keep momentum in the vehicles to minimize the change in velocity.

Case 6 & 7: a touching pair (two additional knots);

$$f_4(t) = \begin{cases} k_l(\delta_1 - t)^3 + k_2(\delta_1 - t)^2 \\ \qquad + k_3(\delta_1 - t) + k4 \\ \qquad\qquad t \in [t_i, \delta_1] \\ m_l(-\delta_1 + t)^3 + m_2(-\delta_1 + t)^2 \\ \qquad + m_3(-\delta_1 + t) + m_4 x \\ \qquad\qquad t \in [\delta_1, \delta_2] \\ g_l(-\delta_2 + t)^3 + g_2(-\delta_2 + t)^2 \\ \qquad + g_3(-\delta_2 + t) + g_4 \\ \qquad\qquad t \in [\delta_2, t_{i+1}]) \end{cases} \tag{2.7}$$

This case of two touching points, Fig. 2.11, that adds two additional knots, δ_1 and δ_2, in the interval. This is similar to cases 1 and 2. This can simulate bumper to bumper traffic while maintaining $v > 0$. Having this oscillation would be the least optimal case due to the drastic changes in velocity to maintain within the upper and lower constraints, $d(t)$ and $e(t)$. Practically, the constraint difference could be very small, that the variation in the case will also be small.

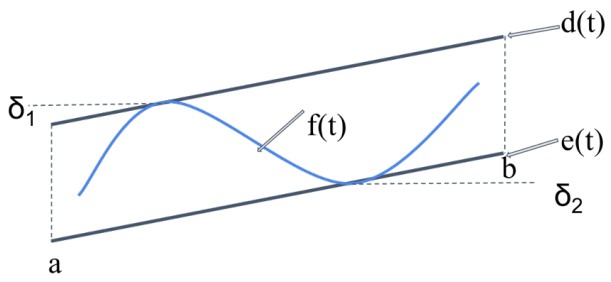

Figure 2.11: Touching pair definition, where $a = t_i$ and $b = t_{i+1}$.

As an example, the candidate solution in case 4 (a single subarc on the lower constraint) is in the form of (2.6) where the subarc on the lower constraint occurs for $t \in [\delta_1, \delta_2]$. In this case all coefficients k_1, k_2, k_3, k_4, m_1, m_2, m_2, m_3, m_4 and parameters δ_1 and δ_2 can be computed by solving linear algebraic equations only. The function (2.2) is computed by adding up the minimum costs from each interval.

2.4 FE Evaluation

This optimal solution technique is implemented in Matlab and is used to compute the optimal Eco-Driving control for the Kalamazoo Arterial and the Kalamazoo Downtown drive cycles. Once the optimal trajectory of the ego vehicle has been determined, the FE is evaluated using established and real-world validated vehicle modeling software. For this study, we chose to use the FASTSim software which is freely available from the National Renewable Energy Laboratory (31).

We are interested in quantifying the results of this technique for several different types of vehicle architecture including Hybrid Electric Vehicles (HEVs), Conventional Vehicles (CVs), and Electric Vehicles (EVs). To meet these criteria, we chose a 2016 Toyota Highlander Hybrid, 2016 Toyota Camry 4 cylinder, and 2016 Tesla Model S60. We have used the Python version of FASTSim for greater flexibility. It uses the drive cycle as an input and provides FE as an output.

The optimal trajectory result will be subsequently shown in distance (mi) versus time (min). In order to apply FASTSim as our validation tool, the second-by-second vehicle velocity time history was inferred from the optimal position trajectory. The road grade was set to zero.

CHAPTER 3

RESULTS

The results of this study are the determined upper and lower constraints, the derived Eco-Driving drive cycle, and the associated FE for the three vehicle models for the Kalamazoo Arterial and the Kalamazoo Downtown routes.

3.1 Optimal Control Solution

The constraints and Eco-Driving drive cycles for the two routes are shown in Figs. 3.1 and 3.2. The lower constraint (red) is the time window just before the traffic turns red and the upper constraint (blue) is the lead vehicle. The optimized trajectory is the green spline which in each time interval, can fall into the seven cases described in section 2.3. Note that Figs. 4 and 5 show two different drive cycles for each route. This is because the initial condition of the ego vehicle route is somewhat arbitrary. For both routes, drive cycle 1 (subfigure a) has an initial slope (velocity of the ego vehicle) determined by the optimizer, whereas drive cycle 2 (subfigure b) has an initial slope chosen to be half the slope of the upper constraint (lead vehicle velocity). This choice is meant to provide distinct results and insights into the optimal solution.

Drive cycles KA1 and KA2 cover a total distance of 3.31 miles in 7.5 minutes. Fig. 4a shows KA1 where the initial slope was chosen by the optimizer. The KA1 trajectory only uses two of the seven possible cases for the optimal solution: case 1 and case 3. The single touching point is located towards the end of the drive cycle at $t = 5.85$ and 6.81 minutes which is the only additional gate other than the 12 fixed gates located at $t = 0$, 0.96, 1.96, 2.97, 3.4, 3.96, 4.4, 5.4, 5.8, 6.8, 7, and 7.44 minutes. The KA2 trajectory also only shows case 1 and case 3. The touching pair is located towards the end of the drive cycle at $t = 6.84$ and 7 minutes which is the only 2 additional gates other than the 12 fixed gates. Comparing the drive cycle 1 and 2, both trajectories

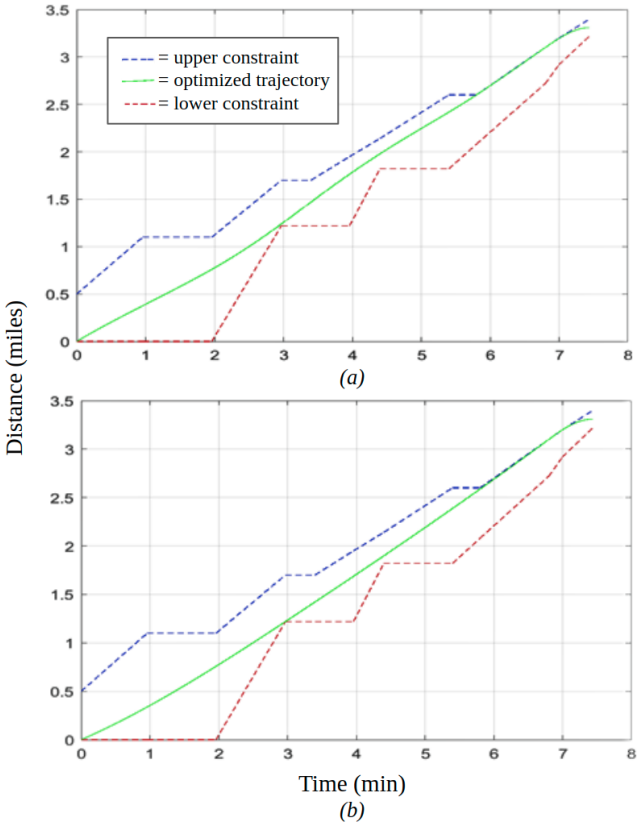

Figure 3.1: Kalamazoo Arterial route results for the Eco-Driving solution with an initial velocity chosen by the optimizer, drive cycle KA1 (a), and an initial velocity assigned as half of the speed limit, drive cycle KA2 (b).

were approximately similar where both had case 1 and case 3 for the possible optimal solution.

Drive cycles KD1 and KD2 cover a total distance of 0.9 miles in 5.9 minutes. Overall this route provides tighter upper and lower constraints for the vehicles trajectory to follow. KD1 again only shows case 1 and case 3. The single touching point is located towards the end of the drive cycle at t =4.4 and 4.6 minutes which is the only additional gate other than the 14 fixed gates located at t =0, 0.2, 0.5, 1.3, 1.5, 1.9, 2.6, 2.9, 3, 3.6, 4.1, 4.4, 4.6, and 5.9 minutes. The KD2 trajectory slightly exceeds the speed limit to make the stop light at t = 1.9 minutes. KD2 also has three cases: case 1, case 2, and case 3. The touching pair is located towards the end of the drive cycle at t = 1.3 and 4.6 minutes which are the only 2 additional gates other than the 14 fixed gates.

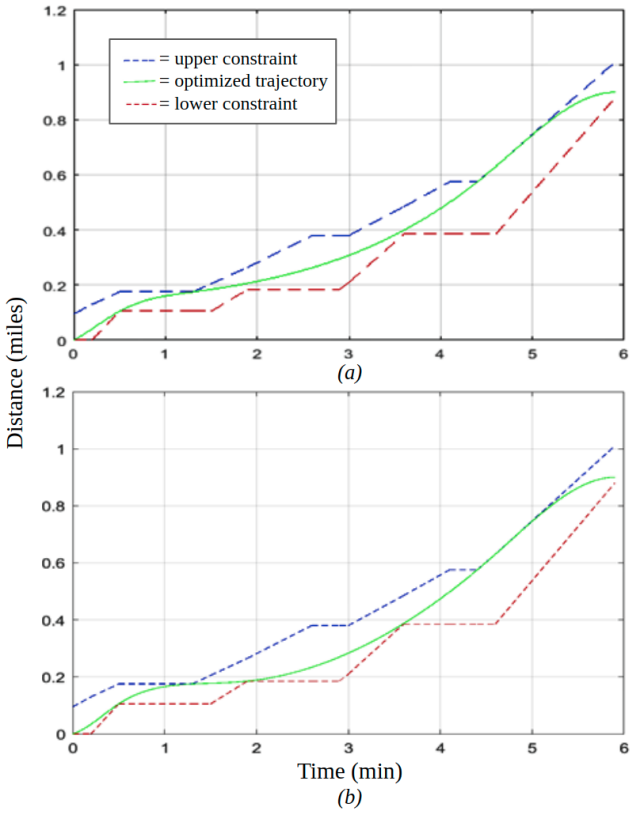

Figure 3.2: Kalamazoo Downtown route results for the Eco-Driving solution with an initial velocity chosen by the optimizer, drive cycle KD1 (a), and an initial velocity assigned as half of the speed limit, drive cycle KD2 (b).

3.2 FE Results

MPGe (miles per gallon gasoline equivalent) and MPG are calculated for all derived drive cycles according to the standard (J1711-201006) (32). Each result is then contrasted with EPA FE measurements for city driving (33) in Table 3.1. Note that the results vary widely depending on the vehicle model used.

Table 3.1 shows a significant energy efficiency increase for all vehicles in both routes when compared to EPA city estimates. Additionally, there is a significant difference in the energy efficiency improvements for the arterial roads vs. downtown. This is because the main-arterial roads are known to have a better FE since they have greater distances between stop lights and their speed limit is higher. Downtown routes have closely spaced traffic lights with lots of acceleration and deceleration. Both the Toyota Camry and the Tesla Model S show FE increases in drive cycle 1 over

Table 3.1: Energy efficiency (i.e. FE) of all drive cycles for an HEV, EV, and CV.

3***Drive Cycle**		**2016 Toyota Highlander Hybrid (HEV) MPG**	**2016 Tesla Model S60 (EV) MPGe**	**2016 Toyota Camry 4cyl (CV) MPG**
2*Main Arterial	Drive-cycle 1	65.5	220.5	48.6
	Drive-cycle 2	65.8	218.5	45.5
2*Downtown	Drive-cycle 1	41.4	243.7	30.6
	Drive-cycle 2	45.0	238.6	30.0
EPA FE (city)		27	98	28

drive cycle 2 in both routes. The Toyota Highlander Hybrid on the other hand shows a significant increase in drive cycle 2 over drive cycle 1 in both routes.

CHAPTER 4

CONCLUSION

This thesis proposed an approach for increasing the energy efficiency of eco-driving vehicles based on the best interpolation in a strip. Two real-world routes were chosen: Kalamazoo Arterial and Kalamazoo Downtown. These routes were converted to distance over time constraints for an optimal control problem to be solvable using the best interpolation in a strip. The optimization problem was programmed into MATLAB software and the MATLAB fmincon tool was used to produce optimized routes for both Kalamazoo Arterial and Kalamazoo Downtown.

Two drive cycles were tested, one drive cycle utilized s_0 equal to half the velocity of the lead vehicle, and the other utilizing the optimizer to determine s_0. The Eco-Driving solution was used as an input to the real-world validated FASTSim models that were used to simulate the performance of an HEV, CV, and EV. FASTSim results were compared to the EPA reported FE for city driving Results. There was a significant increase in MPG and $MPGe_{electric}$ in all drive cycles showing a significant improvement compared to EPA. This increase can yield to future advancement of automotive and allows for improvements in the field of advanced driving-assistant technologies.

Additionally, the requirement that e and d are piecewise linear can be relaxed to e and d being piecewise cubic but the computations become more involved. While an alternative brute force approach to (2.1) involving time discretization and conversion to a quadratic program is also possible, the disadvantages of that route include higher dimensionality of the optimization problem and the potential for "inter-sample" constraint violations (e.g., collisions with lead vehicle or violation of traffic light rules in extreme cases).

Eco-Driving is an important technology to realize sustainable transportation. The method presented here can be used in all levels of vehicle automation provided surrounding vehicle and SPaT data is available. Moreover, Eco-Driving are not only entitled to the improvement of automotive industry technologies but it can reduces the cost of transportation for many industries that

are heavily based on transportation, and help in the reduction of green house gas emissions.

Future work includes measuring the human driver FE of a vehicle along this route, and using real-world measured SPaT data specific to these routes. Utilizing the real world SPaT data and a human driver will help build a high-fidelity model where we can get more accurate results of our application when applied in day-to-day driving activities.

In real vehicles, there are limits on acceleration and velocity. for example, We know that in real world instantaneous acceleration is tied to the vehicle structure and build and its limited by the RpM; vehicles can speed up or slow down only so much in such a short period of time. In our theoretical solution, the acceleration and velocity seems to comply with the speed limit of the routes and it seems that a vehicle can implement the acceleration. For further research, We would like to thoroughly investigate the values of instantaneous acceleration and velocity to be expected in the solution.

Furthermore, we would like to expand beyond the Kalamazoo routes. To be able to expand we will need to perform testing in other states or use simulation tools like FASTsim or the Chassis Dynamometer located in the EEAV lab on different cycles. This will allow us to analyze the different behaviors a driver might encounter on daily basis in addition that it will expand the scope of our research to be applied in the automotive industry.

Last but not least we would like to expand the optimization problem formulation to allow for cubic constraints. Cubic constraints will simulate a better behavior of the (lead vehicle) upper constraint and lower constraint. In real life, we do not anticipate that drivers (in this case, upper and lower constraints) maintain constant speed all the time (linear constraints).

BIBLIOGRAPHY

[1] NHTSA, "Corporate average fuel economy," 2020.

[2] D. Greene and C. Liu, "U.S. oil dependence 2014: Is energy indep. in sight?" *Enrgy Policy*, vol. 85, pp. 126–137, Oct. 2015.

[3] U.S. EIA, "Annual energy outlook 2020," Tech. Rep. AEO2020, 2020.

[4] S. Anenberg, J. Miller, D. Henze, and R. Minjares, "A global snapshot of the air pollution-related health impacts of transportation sect emissions in 2010 and 2015," *Int Council on Clean Trans: Washington, DC*, 2019.

[5] U.S. EPA, "Acid rain, toxic leaded gas, and widespread air pollution? not anymore. thanks to EPA," 2015.

[6] J. Zielinski, R. Andreucci, N. Rajagopalan, and C. Aktas, "Prospects for meeting the corporate average fuel economy standards in the U.S," *Int Council on Clean Trans: Washington, DC*, vol. 136, pp. 466–472, Sep. 2019.

[7] A. B. Schwarzkopf and R. B. Leipnik, "Control of highway vehicles for minimum fuel consumption over varying terrain," *Great Britain*, vol. 11, pp. 279–286, 1977.

[8] A. Dontchev and I. Kolmanovsky, "State constraints in the lin. regulator problem: case study," *Jrnl of opt theory and apps*, vol. 87, no. 2, pp. 323–347, 1995.

[9] E. Ericsson, "Independent driving pattern factors and their influence on fuel-use and exhaust emission factors," *Transportation Research Part D: Transport and Environment*, vol. 6, no. 5, pp. 325–345, 2001.

[10] J. Gondar, M. Earleywine, and W. Sparks, "Analyzing vehicle fuel saving opportunities through intelligent driver feedback," Tech. Rep. 2012-01-0494, 2012.

[11] Z. S. Mohd Azrin Mohd Zulfeki, Jianfeng Zheng and H. X. Liu, "Hybrid powertrain optimization with trajectory prediction based on inter-vehicle-communication and vehicle-infrastructure-integration," *Transp Res Part C: Emerg Technol*, vol. 45, pp. 41–63, 2014.

[12] Z. A. David Baker and T. Bradley, "V2V communication based real-world velocity predictions for improved HEV fuel economy," *SAE Technical Paper*, no. 2018-01-1000, 2018.

[13] P. Michel, D. Karbowski, and A. Rousseau, "Impact of connectivity and automation on vehicle energy use," SAE Tech Paper, Tech. Rep., 2016.

[14] Y. Huang, E. Ng, J. Zhou, and Surawski, "Eco-driving technology for sustainable road transport: A review," *Renewable Sust Energy Rev.*, vol. 93, pp. 596–609, Oct. 2018.

[15] C. Rödel, S. Stadler, A. Meschtscherjakov, and M. Tscheligi, "Towards autonomous cars: The effect of autonomy levels on acceptance and user experience," *Renewable. Sust Energy Rev.*, pp. 1–8, Sep. 2014.

[16] A. Mohan, S. Sripad, P. Vaishnav, and V. Viswanathan, "Trade-offs between automation and light vehicle electrification," *Nature Energy*, vol. 5, pp. 543–549, 2020.

[17] U.S. DOE, "Connected and automated vehicles capstone report," U.S. DOE Office of Enrgy Eff. & Ren. Enrgy, Tech. Rep., 2020.

[18] S. Mandava, K. Boriboonsomsin, and M. Barth, "Arterial velocity planning based on traffic signal information under light traffic conditions," ser. AutomotiveUI '14. 2009 12th Int IEEE Conf on Intelligent Trans Syst, Sep. 2009, pp. 1–6.

[19] M. R. Amini, X. Gong, Y. Feng, H. Wang, I. Kolmanovsky, and J. Sun, "Sequential opt of speed, thermal load, and power split in connected hevs," 2019, pp. 4614–4620.

[20] Z. Yang, Y. Feng, X. Gong, D. Zhao, and J. Sun, "Eco-Trajectory planning with consideration of queue along congested corridor for hybrid electric vehicles," *Transp. Res. Rec.*, vol. 2673, no. 9, pp. 277–286, Sep. 2019.

[21] S. Iliev, E. Rask, K. Stutenberg, and M. Duoba, "Eco-Driving strategies for different powertrain types and scenarios," *SAE Int Jrnl of Advances and Current Practices in Mobility*, vol. 2, no. 2019-01-2608, pp. 945–954, 2019.

[22] S. Bae, Y. Kim, J. Guanetti, F. Borrelli, and S. Moura, "Design and implementation of eco adaptive cruise control for autonomous driving with communication to traffic lights," in *2019 ACC*, 2009, pp. 4628–4634.

[23] N. Prakash, G. Cimini, A. Stefanopoulou, and M. Brusstar, "Assessing fe from automated driving: Influence of preview and velocity constraints," in *ASME 16 Dyn Sys and Ctrl Conf*. ASME dig coll, 2017.

[24] M. Egerstedt and C. Martin, *Control Theoretic Splines: Opt. Cont, Stats, Path Planning*. Princeton U, 2009.

[25] A. Dontchev, "Best interpolation in a strip," *J. Approx. Theory*, vol. 73, no. 3, pp. 334–342, Jun. 1993.

[26] A. Dontchev and I. Kolmanovsky, "Best interpolation in a strip II: Reduction to unconstrained convex optimization," *Comp Optim App*, vol. 5, no. 3, pp. 233–251, May 1996.

[27] N. Prakash, A. Stefanopoulou, A. Moskalik, and M. Brusstar, "Use of the hypothetical lead (HL) vehicle trace: A new method for evaluating fuel consumption in automated driving," in *2016 ACC*, Jul. 2016, pp. 3486–3491.

[28] ——, "On the effectiveness of hybridization paired with Eco-Driving," pp. 4635–4640, Jul. 2019.

[29] P. Koonce, L. Rodegerdts, K. Lee, S. Quayle, S. Beaird, C. Braud, J. Bonneson, P. Tarnoff, and T. Urbanik, "Traffic signal timing manual," 2008.

[30] NACTO, "Urban street design guide," 2013.

[31] A. Brooker, J. Gonder, L. Wang, E. Wood, S. Lopp, and L. Ramroth, "FASTSim: A model to estimate vehicle efficiency, cost and performance," 2015.

[32] SAE, “Recommended practice for measuring the exhaust emissions and fuel economy of hevs, including plug-in hybrid vehicles,” Tech. Rep., 2010.

[33] U.S. EPA, “Plug-in hybrid electric vehicle - learn more about the new label,” 2021.

APPENDIX

Matlab Code

```
%{
strip optimization main
Input: csv file with 6 columns of a,b,lower m, lower b, upper m, upper b

Must set Y and S boundary values at endpoints of interval when not an
optimization parameter
%}

% housekeeping
close all;
clear;

% setup
csvfname= 'constraintsdatacleanedformatlab.csv';
Ybv_t0= 0; % y value at the start time
Ybv_tf= 0.9; % y value at the final time
Sbv_tf= 0; % dy/dt (slope) at the final time

% read and process data
[knots,id,l,lb,n,u,ub]= ecodriving_initialize(csvfname);
plot_constraints

% modify lb and ub for slope as optimization value at t_a, firt time point
lb= [lb,l.cf(1,3)];
ub= [ub,u.cf(1,3)];

% boundary values
Ybv= [Ybv_t0,Ybv_tf]; % position at initial and final point
Sbv= Sbv_tf; % slope at final point
% slope at final time set to zero for zero velocity

% initial guess
S0= zeros(1,n-2);
Y0= (lb(id.SY2Y)+ub(id.SY2Y))/2;
s0= (lb(end)+ub(end))/2;
SYs0= [S0,Y0,s0];

% additional paramters
toll= 1e-12;

% optimization
opt_fmincon= optimset;
opt_fmincon.Algorithm= 'sqp';
opt_fmincon.Display= 'iter';
opt_fmincon.MaxFunEvals= 5000;

% optimization
[SYs,fval,flg_exit,info]= fmincon( ...
    @(SYs) cost_splines_s0(SYs,id,knots,l,n,u,Sbv,toll,Ybv), ...
    SYs0,[],[],[],[],lb,ub,[],opt_fmincon);

% get data
[cost, cons, splines]= cost_splines_s0(SYs,id,knots,l,n,u,Sbv,toll,Ybv);

% plot
plot_splines;

function [knots,id,l,lb,n,u,ub]= ecodriving_initialize(csvfname)
%{
extract information for strip optimization

id: indexing to unwrap S and Y during optimization
lb: lower bound on Y, prevents solver from violating constraints at knots
ub: upper bound on Y, prevents solver from violating constraints at knots

%}

% check file name
```

```
if (~endsWith(csvfname,'.csv','IgnoreCase',true))
    csvfname= [csvfname,'.csv'];
end

% load data
csvdata= csvread(csvfname);
% plot_csvdata(csvdata)

% number of intervals
n_int= numel(csvdata(:,1));
n= n_int+1;

% knots
knots= [csvdata(:,1);csvdata(end,2)];

% initialize
l= struct;
u= struct;
l.cf= zeros(n_int,4);
u.cf= zeros(n_int,4);

% strip bound equations are defined relative to the last point
% shift data
l.cf(1,3:4)= csvdata(1,3:4);
u.cf(1,3:4)= csvdata(1,5:6);
for ii=2:n_int
    b_l= polyval(csvdata(ii-1,3:4),knots(ii));
    m_l= csvdata(ii,3);
    b_u= polyval(csvdata(ii-1,5:6),knots(ii));
    m_u= csvdata(ii,5);
    l.cf(ii,3:4)= [m_l,b_l];
    u.cf(ii,3:4)= [m_u,b_u];
end

% index and numbers
id= struct;
id.SY2S= 1:(n-2);
id.SY2Y= (n-2+1):(2*(n-2));

% bounds
lb= -Inf(1,2*(n-2));
ub= Inf(1,2*(n-2));

% set Y bounds
for ii=2:(n-1)
    % lower
    tmp1= polyval(l.cf(ii-1,:),knots(ii)-knots(ii-1));
    tmp2= polyval(l.cf(ii,:),0);
    lb(id.SY2Y(ii-1))= max(tmp1,tmp2);

    % upper
    tmp1= polyval(u.cf(ii-1,:),knots(ii)-knots(ii-1));
    tmp2= polyval(u.cf(ii,:),0);
    ub(id.SY2Y(ii-1))= min(tmp1,tmp2);
end

end

function [cost, cons, splines]=cost_splines_s0(SYs,id,knots,l,n,u,Sbv,toll,Ybv)
% Sbv, Ybv: S and Y bounday values at a and b
% l,u: lower and upper constraints (use l.cf(i,:), u.cf(i,:) to get coefficients for the ith
    interval)
% Sbv only includes final slope

% unwrap S and Y
S= SYs(id.SY2S);
Y= SYs(id.SY2Y);
```

```
% unwrap s0
s0= SYs(end);

% total position and slope values
S= [s0,S,Sbv];
Y= [Ybv(1),Y,Ybv(end)];

% spline calculation
[cost, cons, splines]= calc_splines(knots,l,n,u,S,toll,Y);

end

function [cost, cons, splines]=calc_splines(knots,l,n,u,S,toll,Y)
% all spline data given knots and slopes

% intial values
cost =  0;
cons= -Inf;

% storage
splines= struct;
splines.X= cell(1,n-1);
splines.cf= cell(1,n-1);
splines.case= cell(1,n-1);

% step through intervals
for ii=1:n-1

    %there is a total of n-1 intervals
    a= knots(ii);
    b= knots(ii+1);
    c= Y(ii);
    d= Y(ii+1);
    s1= S(ii);
    s2= S(ii+1);
    li= l.cf(ii,:);
    ui= u.cf(ii,:);

    [inc_cost1, inc_cons1, cf1] =  case1(a,b,c,d,li,ui,s1,s2,toll);
    if (inc_cons1<=toll)
        % unconstrained cubic spline is the solution
        splines.X{ii}= [a,b];
        splines.cf{ii}= cf1(:)';
        splines.case{ii}= 1;
        cost= cost+inc_cost1;
        cons= max(cons,inc_cons1);

    else

        cands=[];
        [inc_cost2l,inc_cons2l,del2l,k2l,m2l]=case2l(a,b,c,d,li,ui,s1,s2,toll);
        if (inc_cons2l<=toll)
            cands=[cands;21,inc_cost2l];
        end

        [inc_cost2u,inc_cons2u,del2u,k2u,m2u]=case2u(a,b,c,d,li,ui,s1,s2,toll);
        if (inc_cons2u<=toll)
            cands=[cands;22,inc_cost2u];
        end

        [inc_cost3l,inc_cons3l,del3l,k3l,m3l,llr3]=case3l(a,b,c,d,li,ui,s1,s2,toll);
        if (inc_cons3l<=toll)
            cands=[cands;31,inc_cost3l];
        end

        [inc_cost3u,inc_cons3u,del3u,k3u,m3u,uur3]=case3u(a,b,c,d,li,ui,s1,s2,toll);
        if (inc_cons3u<=toll)
            cands=[cands;32,inc_cost3u];
```

```
        end

        [inc_cost4lu,inc_cons4lu,del4lu,k4lu,m4lu,f4lu]=case4lu(a,b,c,d,li,ui,s1,s2,toll);
        if (inc_cons4lu<=toll)
            cands=[cands;41,inc_cost4lu];
        end

        [inc_cost4ul,inc_cons4ul,del4ul,k4ul,m4ul,f4ul]=case4ul(a,b,c,d,li,ui,s1,s2,toll);
        if (inc_cons4ul<=toll)
            cands=[cands;42,inc_cost4ul];
        end

        if isempty(cands)
            % no feasible solution exists (abnormal case)
            % use unconstrained cubic spline solution
            splines.X{ii}= [a,b];
            splines.cf{ii}= cf1(:)';
            splines.case{ii}= -1;
            cost= cost+inc_cost1;
            cons= max(cons,inc_cons1);
        else
            [vmin,imin]=  min(cands(:,2)); %select minimum cost solution from available
                options
            if (cands(imin,1)==21)
                splines.X{ii}= [a,del2l,b];
                splines.cf{ii}= [k2l(:)';m2l(:)'];
                splines.case{ii}= 21;
                cost= cost+inc_cost2l;
                cons= max(cons,inc_cons2l);

            elseif (cands(imin,1)==22)
                splines.X{ii}= [a,del2u,b];
                splines.cf{ii}= [k2u(:)';m2u(:)'];
                splines.case{ii}= 22;
                cost= cost+inc_cost2u;
                cons= max(cons,inc_cons2u);

            elseif (cands(imin,1)==31)
                splines.X{ii}= [a,del3l,b];
                splines.cf{ii}= [k3l(:)';l1r3(:)';m3l(:)'];
                splines.case{ii}= 31;
                cost= cost+inc_cost3l;
                cons= max(cons,inc_cons3l);

            elseif (cands(imin,1)==32)
                splines.X{ii}= [a,del3u,b];
                splines.cf{ii}= [k3u(:)';uur3(:)';m3u(:)'];
                splines.case{ii}= 32;
                cost= cost+inc_cost3u;
                cons= max(cons,inc_cons3u);

            elseif (cands(imin,1)==41)
                splines.X{ii}= [a,del4lu,b];
                splines.cf{ii}= [k4lu(:)';m4lu(:)';f4lu(:)'];
                splines.case{ii}= 41;
                cost= cost+inc_cost4lu;
                cons= max(cons,inc_cons4lu);

            elseif (cands(imin,1)==42)
                splines.X{ii}= [a,del4ul];
                splines.cf{ii}= [k4ul(:)';m4ul(:)';f4ul(:)'];
                splines.case{ii}= 42;
                cost= cost+inc_cost4ul;
                cons= max(cons,inc_cons4ul);
            end
        end
    end
end
```

```
end

function [cost, cons, splines]=cost_splines(SY,id,knots,l,n,u,Sbv,toll,Ybv)
% Sbv, Ybv: S and Y bounday values at a and b
% l,u: lower and upper constraints (use l.cf(i,:), u.cf(i,:) to get coefficients for the ith
     interval)

% unwrap S and Y
S= SY(id.SY2S);
Y= SY(id.SY2Y);

% total position and slope values
S= [Sbv(1),S,Sbv(end)];
Y= [Ybv(1),Y,Ybv(end)];

% spline calculation
[cost, cons, splines]= calc_splines(knots,l,n,u,S,toll,Y);

end

%{
plot the lower and upper bounds and the 3rd order splines

execute in optimization results workspace
%}

% setup

figure;
hold on;

% lower and upper constraints
for ii=1:(n-1)
    % lower
    plot(knots(ii:ii+1),polyval(l.cf(ii,:),[0,knots(ii+1)-knots(ii)]),'r--');

    % upper
    plot(knots(ii:ii+1),polyval(u.cf(ii,:),[0,knots(ii+1)-knots(ii)]),'b--');
end

slope = struct;
% spline segments
for ii=1:(n-1)

    % number of segements in the interval
    n_seg= numel(splines.cf{ii}(:,1));

    for jj=1:n_seg

        tmp1= linspace(splines.X{ii}(jj),splines.X{ii}(jj+1),20);
        plot(tmp1,polyval(splines.cf{ii}(jj,:),tmp1-splines.X{ii}(jj)),'g-');

          %if  jj < 20
             % slope = (polyval(splines.cf{ii}(jj+1,:),tmp1-splines.X{ii}(jj+1)))-(polyval(
                 splines.cf{ii}(jj,:),tmp1-splines.X{ii}(jj)))/(tmp1-splines.X{ii}(jj+1)-
                 tmp1-splines.X{ii}(jj));
             % fprintf();
         % end
    end


end
%extracting the xy data from the plot
h = findobj(gca,'Type','line');
x= get(h,'Xdata');
y= get(h,'Ydata');
```

```
%storing the data in xyarr, the for loop doesnt add the last the point data
iii = 1;
% x{13,1}(20)
for i= 13:-1:1

    for ii= 1:1:19

        xyarr(iii,1)= x{i,1}(ii);
        xyarr(iii,2)= y{i,1}(ii);
        iii = iii+1;

    end

end

xyarr(iii,1)= x{1,1}(20);
xyarr(iii,2)= y{1,1}(20);

%finding the slope (velocity) and storing it in the 3rd col of xyarr

for i=1:1:iii
    if i < iii
    xyarr(i,3) =( xyarr(i+1,2)-xyarr(i,2))/(xyarr(i+1,1)-xyarr(i,1));
    xyarr(i,4) = xyarr(i,3)*60;
    end
end

%finding the aceleration and storing it in the 5th col of xyarr
for i=1:1:iii
    if i < iii
    xyarr(i,5) =( xyarr(i+1,3)-xyarr(i,3))/(xyarr(i+1,1)-xyarr(i,1));
    xyarr(i,6)= xyarr(i,5)*3600;
    end
end
xlswrite('downtownresults.xls',xyarr);
writematrix(xyarr,'resultsdowntown.csv');

% complete
hold off;
grid on;
box on;
ylabel('Distance');
xlabel('Time');
```